Electronic Supplementary Material (ESI) for Chemical Communications
This journal is © The Royal Society of Chemistry 2015

Supporting information

Highly proton-conducting, methanol-blocking Nafion composite membrane enabled by surface-coating crosslinked sulfonated graphene oxide

Guangwei He[ab], Xueyi He [ab], Xinglin Wang [a], Chaoyi Chang [a], Jing Zhao [ab], Zongyu Li[ab], Hong Wu[ab], and Zhongyi Jiang*[ab]

[a] Key Laboratory for Green Chemical Technology of Ministry of Education, School of Chemical Engineering and Technology, Tianjin University, Tianjin 300072, China.

[b] Collaborative Innovation Center of Chemical Science and Engineering (Tianjin), Tianjin 300072, China

Experimental Section

Materials

Nafion 212 membrane was obtained from DuPont (USA). 1, 4-phenylenediamine-2-sulfonic acid (PDASA) was purchased from Beijing Bailingwei Co., Ltd. (China). PDASA was transformed into Na^+ form in water using NaOH at equal molar ratio before use because PDASA is unable to dissolve in water. Polyethyleneimine (PEI, M.W. 70,000, 50% aqueous solution) was obtained from Aladdin, China. Natural

flake graphite (2500 mesh) was purchased from Qingdao Tianhe Graphite Co. Ltd. (Shandong, China). Sodium hydroxide (NaOH), concentrated sulfuric acid (H_2SO_4) and potassium permanganate ($KMnO_4$) were purchased from Tianjin Kewei Ltd. (Tianjin, China). All the reagents were of analytical grade and used as received. Deionized water was used throughout the experiments.

Preparation of the graphene oxide (GO)

GO dispersion was synthesized according to the modified Hummers method[1], which was described in detail in our previous study[2]. 115 mL of 98 wt% H_2SO_4 was added into a flask at 0 ^oC. Then, 5 g of graphite powder and 2.5 g of $NaNO_3$ were added under stirring, followed by adding 15 g of $KMnO_4$ slowly under a temperature below 5 ^oC. After stirring for 2 h, the mixture was transferred into an oil bath at about 35 ^oC. After 30 min, 230 mL of water was added. Then the temperature of oil bath was kept at 98 ^oC for 3 h. Subsequently, the mixture was poured into a large amount of deionized water, followed by adding 30 mL of H_2O_2. Finally, the mixture was washed with HCl solution, and then washed with water until the pH reached 7.0. The GO aqueous solution could be obtained by dispersing above product in water under ultrasonic treatment for one hour. The GO aqueous solution was centrifuged at 8,000 rpm for 40 min to remove aggregated GOs or large sized GOs.

Preparation of the composite membranes

The GO-PDASA (Na^+ form) mixed aqueous solution (GO@PDASA (Na^+)) in water containing 1 mg/mL of GO and 0.01 M of PDASA was prepared. Nafion 212

support was immersed in water, and then carefully attached onto a glass plate, which was placed on a spin coater. The composite membrane was prepared by the following steps according to the reported method[3]: (1) The glass plate was spun at 3,000 rpm (this speed was used in all the steps), and 1 mL of PEI aqueous solution (1 mg/mL) was dropped on the center of the spinning membrane, which was kept spinning for 60 s. Then, the membrane was washed with water to remove the physically adsorbed PEI through dropping water on the spinning membrane; (2) 1 mL of GO solution (1 mg/mL) was dropped on the center of the spinning membrane which was kept spinning for 60 s; (3) 1 mL of GO@PDASA (Na^+) solution was dropped on the center of the spinning membrane which was kept spinning for 60 s. The step of (3) was repeated n times; (4) The resulting membrane was heated at 80 ^oC for 12 h to induce the crosslinking between amine group (in PEI and PDASA) and epoxy group (in GO)[4]; (5) The membrane was immersed in 1 M of H_2SO_4 solution for 24 h, followed by washing with water until the pH of 7 was reached. The resulting composite membrane was designated as Nafion/GO@PDASA-n. Nafion/GO-n membrane was prepared for comparison using the same method described for Nafion/GO@PDASA-n except using 1 mL of GO solution (1 mg/mL) in the step of (3). PEI was first coated on Nafion support membrane to introduce a high density of amine groups, which could render abundant electrostatic interactions (between Nafion and amine group, and between amine group and carboxyl group) and covalent bonds (between amine group and epoxy group of GO) between the Nafion support and GO film.

Characterizations

Cross-section morphology of the membrane was observed by field emission scanning electron microscope (FESEM, Nanosem 430) after the membrane being freeze-fractured in liquid nitrogen and then sputter-coated with a thin gold layer. To clearly observe the GO@PDASA film, the GO@PDASA solution was spin-coated on Nafion support for 80 times.

The morphology of GO was imaged by atomic force microscope (AFM, CSPM 5000) at room temperature.

FTIR spectra of the GO sample were determined by a BRUKER Vertex 70 FTIR spectrometer equipped with a horizontal attenuated transmission accessory at room temperature.

The chemical compositions of GO@PDASA film (about 80 nm) on Nafion support were determined by X-ray photoelectron spectroscopy (XPS, Kratos Axis Ultra DLD) at room temperature with a monochromatic Al Kα source and a charge neutralizer. The probe depth of XPS is about 10nm.

Wide-angle X-ray diffraction (XRD) was performed at room temperature to detect the crystallization property of dry GO sample, Nafion 212 membrane and the modified surface of the composite membrane using a D/MAX-2500 X-ray diffractometer (CuK α).

Measurement of proton conductivity, gas permeability, methanol permeability and water uptake

Proton conductivity of the membranes under the condition of 30-80 °C and 100% RH was tested by two-point probe alternating current (AC) impedance spectroscopy with a frequency range of 10^6−1 Hz using an electrode system connected with frequency response analyzer (FRA, Compactstat, IVIUM Tech.).[5] Both proton conductivities in in-plane direction and through-plane direction were measured using parallel platinum electrodes and vertical stainless steel electrodes, respectively.[6] Proton conductivity in in-plane direction was tested after the samples were fully hydrated in water and equilibrated in a temperature-controlled water-bath chamber for 1 hour. Proton conductivity in through-plane direction was tested in water. Proton conductivity (σ, S cm^{-1}) was calculated according to the relationship: $\sigma = l/AR$, where R is the resistance, A is the cross-section of the sample, and l is the length between the electrodes.

Gas permeabilities of H_2 and CH_4 through the membranes were measured for elucidating the variations of GO's interlayer spacing according to our previous studies.[7] The membranes were measured by a constant volume/variable pressure apparatus shown in our previous study to obtain the permeability data of each probe molecule. The measurements were tested at 30 °C and 1 bar of the high-pressure side after being evacuated for 8 h to remove the possibly dissolved species in membranes.

The methanol permeability was measured at room temperature (30 °C) using a diffusion cell, in which the methanol solution (2 M or 5 M) permeates through the sandwiched membrane into the water compartment.[8, 9] The concentration of methanol

that permeated into the water compartment was determined by a gas chromatography (Agilent 6820) equipped with a Thermal Conductivity Detector (TCD) and a DB624 column. The measurement method was described in detail in our previous study.[10]

Rectangular samples were dehydrated at 80 °C till constant weight and the weight (W_{dry}) was tested. Subsequently, the samples were immersed in water at 30 °C until full hydration and the weight (W_{wet}) was tested. The measurements were repeated three times to obtain an average value. The water uptake was calculated by the equations: water uptake (%) = $(W_{wet}–W_{dry})/W_{dry} \times 100$.

Single cell measurement

The membrane electrode assembly (MEA) was made by sandwiching a Nafion® 212 membrane or a composite membrane between gas-diffusion Electrodes by hot pressing method (conditions: 135 °C and 4 MPa for 5 min.).[11] The Pt-Ru/C catalyst (40 wt% Pt and 20 wt% Ru, Johnson Matthey) and the Pt/C catalyst (60 wt% Pt, Johnson Matthey) were used as the anodic and cathodic catalysts, respectively. The catalyst loading was 1 mg cm^{-2} for the anode and 0.6 mg cm^{-2} for the cathode. The ionomer (Nafion) loading was 30 wt% for both cathode and anode. The performance of the single cell was measured at 60 °C using a single cell with an effective electrode area of 6.25 cm^2. 2 M CH_3OH solution was fed to the anode with a flow rate of 5 mL min^{-1} and humidified oxygen was supplied to the cathode with a flow rate of 150 mL min^{-1} at 0.1 MPa.

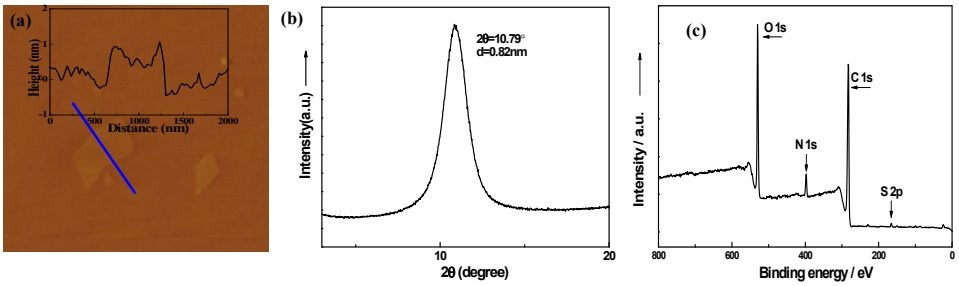

Fig. S1 (a) AFM image of GO; (b) XRD pattern of GO powder at dry state; (c) XPS spectra of GO@PDASA film.

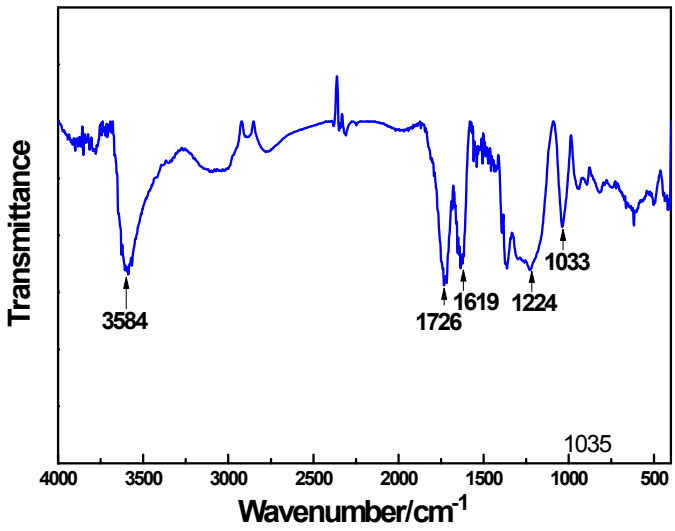

Fig. S2 FTIR spectrum of GO sample.

The characteristic absorption bands of GO are appeared at 1726 cm^{-1} (C=O stretching vibration), 1619 cm^{-1} (C=C stretching vibration), 1224 cm^{-1} (C-O stretching vibration in epoxy group), 1033 cm^{-1} (C-O stretching vibration in C-OH group) and 3475 cm^{-1} (O-H stretching vibration).[12] These characteristic absorption bands demonstrate the presence of carboxyl, epoxy and hydroxyl groups on GO.

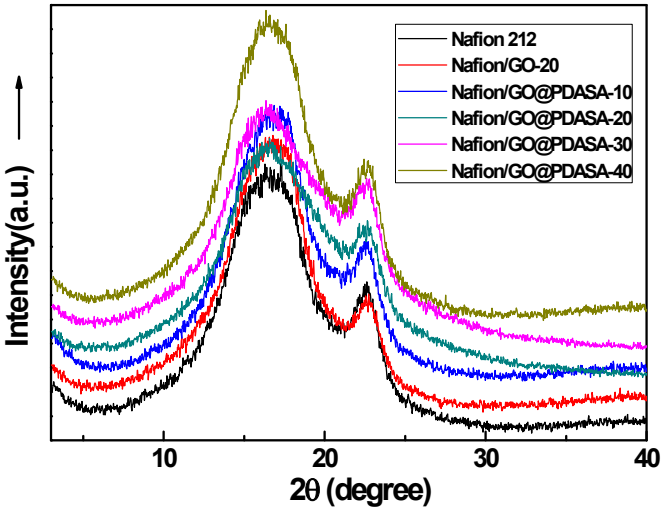

143

144 **Fig. S3** XRD patterns of Nafion 212 and composite membrane at dry state.

145

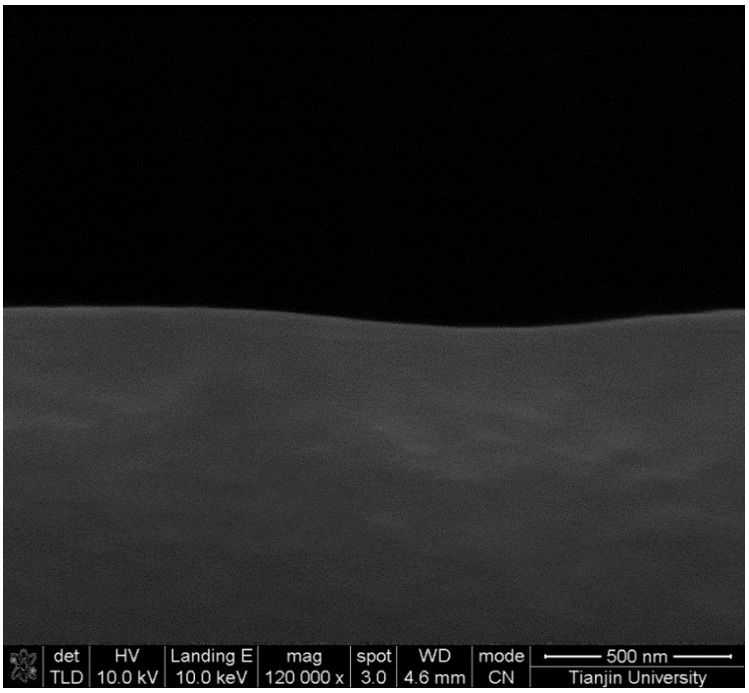

146

147 **Fig. S4** SEM image of cross-sectional sample for Nafion 212 membrane.

148

149 Table S1 Water uptake of the membranes at 30 °C.

Nafion 212	Nafion/GO@PDASA-5	Nafion/GO@PDASA-10	Nafion/GO@PDASA-20	Nafion/GO@PDASA-30	Nafion/GO@PDASA-40	Nafion/GO -20
0.164	0.161	0.162	0.164	0.165	0.162	0.157

150 The water uptakes of all the membranes are nearly identical. The differences of

151 water uptakes are in the range of error (5%). The GO or GO@PDASA membranes on

the Nafion support have negligible thickness (< 40 nm), and thus they have less influence on the water uptake of the composite membranes.

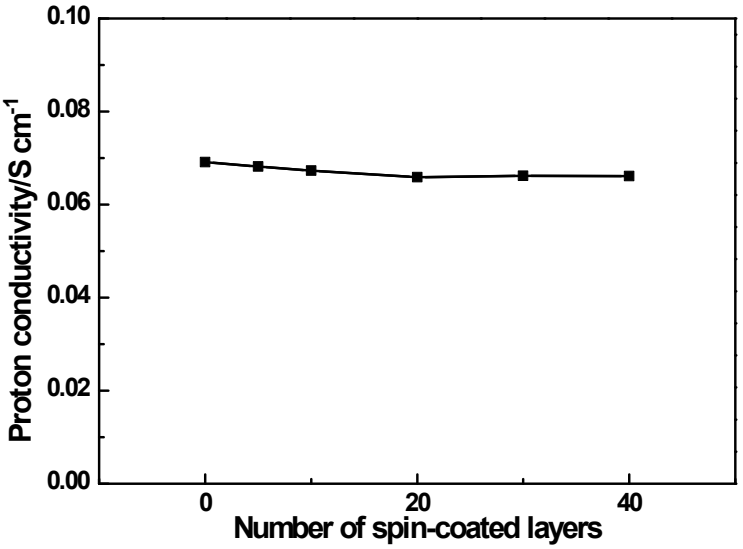

Fig. S5 Proton conductivity (through-plane) of Nafion/GO@PDASA membrane as a function of the number of spin-coated GO@PDASA layers.

The through-plane proton conductivity of the composite membrane shows only 4.3% decrease with increasing the number of GO@PDASA layer from 0 to 40. This tendency of through-plane proton conductivity is in accordance with that of in-plane proton conductivity (Fig. 3b). Because the much larger interfacial regions between the membrane and the electrodes for the through-plane method, the interfacial resistance is larger in comparison with that for the in-plane method. Thus, the proton conductivity in the through-plane direction is always lower than that in the in-plane direction, and the in-plane conductivity is much more accurate.[13] For this reason, in-plane conductivity is more frequently presented for PEMs.

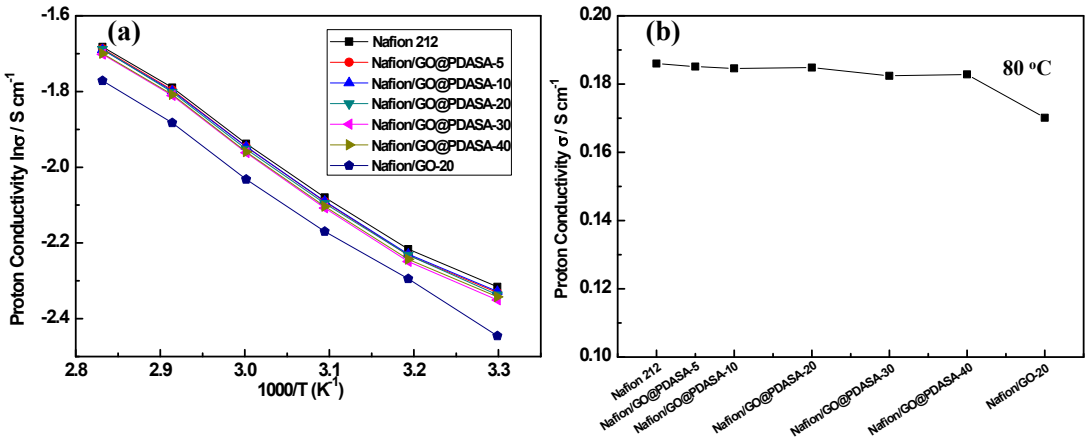

168

169 Fig. S6 (a) Temperature-dependent proton conductivities of the membranes at
170 100% RH; (b) Comparison of the proton conductivities at 80 °C and 100%RH.

171 According to the temperature-dependent proton conductivities in Fig. S5a, the
172 Arrhenius activation energies (Ea) are calculated. The Ea values of Nafion 212,
173 Nafion/GO@PDASA-5, Nafion/GO@PDASA-10, Nafion/GO@PDASA-20,
174 Nafion/GO@PDASA-30, Nafion/GO@PDASA-40, and Nafion/GO-20 are 11.65,
175 11.87, 11.75, 11.88, 11.95, 11.84, and 12.06 kJ mol^{-1}, respectively. The slight
176 variation of Ea indicates that the coating of GO or GO@PDASA membrane on
177 Nafion support does not remarkably changes the proton transport mechanism of the
178 resulting composite membrane. This may account for the small difference of proton
179 conductivities between Nafion and composite membranes. The proton conductivities
180 at 80 °C (Fig. S5b) show nearly identical variation tendency as those at 30 °C (Fig. 3a).
181 The proton conductivities of Nafion, Nafion/GO@PDASA-20 and Nafion/GO-20 at
182 80 °C are 0.186, 0.1848 and 0.1701 S cm^{-1}, respectively.

183

184

185

Table S2 Comparison of proton conductivity, methanol permeability and selectivity for membranes in literature and in this study.

Entry	Membrane	Proton conductivity / mS cm^{-1}	Methanol permeability $\times 10^7/cm^2\ s^{-1}$	Selectivity $\times 10^4$ /S s cm^{-3}	Methanol Concentration /mol L^{-1}	Ref.
1	Nafion/GO@PDASA-20	96.6	1.32	73.18	2	This work
2	Nafion/GO -20	86.7	12.56	6.90	2	This work
3	Nafion/PDDA@PSS-8bilayers	106	decreased by 30%	-	2	[14]
4	Nafion/unbalanced charged polyampholyte-20bilayers	66	5.7	11.58	1	[15]
5	Nafion/PDDA@PWA-4 bilayers	38	10	3.8	2	[11]
6	Nafion/PAH@PSS-5 bilayers	18.4	4.88	3.77	5	[16]
7	Nafion/PAH@PVS-10 bilayers	78	3.44	22.67	10	[17]
8	Nafion/sulphonated PVdF-co-HFP@PBI	15.1	4.92	3.07	2	[8]
9	SPEEK/CS layer (11.5μm)	39	2.81	13.88	1	[18]
10	LbL electrospun composite membrane	7	0.97	7.22	-	[19]
11	Nafion/PDA layer	60	5.6	10.71	2	[20]
12	Nafion/silica layer	58	1.69	34.32	2	[21]
13	Nafion/silica layer	30	0.3	100	2	[21]
14	Sandwich-shaped Nafion/GO-80 layers (800 nm)	14	0.67	20.90	2	[22]
15	Nafion/GO@PDDA-2bilayers	24	13	1.85	2	[23]
16	Nafion/GO layer (800 nm)	23.5	9.28	2.53	1	[24]
17	Nafion/SDBS-GO-8 wt%	93.8	9.5	9.87	1	[25]
18	Nafion/SGO	70	8.09	8.65	12	[26]
19	Nafion/AMPS-MMT-3 wt%	81.7	0.91	89.78	-	[27]
20	Nafion/Cloisite 10A-3 wt%	60	1.1	54.54	3	[28]
21	Nafion/MMT-POPD400-PS-3 wt.%	113	15	7.53	10	[29]
22	Nafion/carbon	126	7.9	15.95	2	[30]
23	Nafion/zeolite	86.3	2.28	37.85	14	[31]

24	SPEEK/silica nanotube	100	3.6	27.78	2	[32]
25	SPPPO/hollow glass microsphere-15wt%	21.2	3.41	6.22	10	[33]
26	SPEEK/zirconium oxide	5	0.91	5.49	1	[34]
27	Dually cross-linked SPAES	86	3.5	24.57	10	[35]
28	Crosslinked SPAES	45	5	9	10	[36]
29	Semi-Interpenetrating polymer network	80	3.5	22.86	2	[37]
30	Crosslinked PVA/PAA/silica	12	2.1	5.71	2	[38]
31	Crosslinked PVA	15	3.3	4.54	2	[39]
32	GO membrane	4	0.32	12.5	5	[40]
33	SPAES block copolymer	150	14	10.71	0.5	[41]
34	SPAES block copolymer	190	25	7.6	0.5	[41]
35	SPAES block copolymer	100	11	9.09	0.5	[41]
36	Sulfonated poly(St-b-EE-r-BDE-b-St)	45	26	1.73	1.5	[42]
37	Sulfonated poly(St-b-EE-r-BDE-b-St)	23	8.2	2.80	1.5	[43]
38	Sulfonated poly(St-b-IB-b-St)	19	1.5	12.67	2	[44]
39	Nafion 212	98.7	18.68	5.28	2	This work

Table S2 shows the performance of six types of membranes: (i) composite membranes (1-16); (ii) organic-inorganic hybrid membranes (17-23); (iii) crosslinked membranes (24-28); (iv) GO membrane (29); (v) block copolymer membranes (30-35) and (vi) Nafion 212 membrane (36). Among them, the following two strategies are more frequently adopted to improve the methanol-blocking properties: (1) Composite membrane: surface-modifying the membrane with a thin methanol-barrier layer. This innovative membrane configuration provides the probability of combining the ostensibly contradictory properties in a heterogeneous system. However, the proton conductivity usually reduces due to the concomitant deterioration of proton-transport

pathway (destructing the continuous sulfonated acid-containing channels). For example, Lin prepared GO-laminated Nafion dual-layer membrane, showing a 70% decrease of methanol permeability at a sacrifice of 22% of proton conductivity.[24] This is probably ascribed to that the thick GO layer (800 nm) without appropriate chemical microenvironment blocks the transport of protons. The conductivity of GO membrane was reported to be only 0.004 S cm^{-1} because the presence of carboxy, hydroxy and epoxy groups could not donate a high concentration of dissociated H^+ (ionic conductivity $\propto$ ion mobility $\times$ ion concentration).[45] (2) Hybrid membrane. The incorporation of nanoparticles could make the transport channels more tortuous or decrease the free volume of membranes, leading to reduced methanol permeability. However, such morphological transformation of channels usually cause concomitant decline of proton conductivity.

Table S3. Proton conductivity, methanol permeability and selectivity of Nafion 212 membrane and the composite membranes in this study.

Membrane	Proton conductivity / mS cm^{-1}	Methanol permeability (2 M[a]) $\times 10^7/cm^2\ s^{-1}$	Methanol permeability (5 M[b]) $\times 10^7/cm^2\ s^{-1}$	Selectivity $\times 10^4$ (2 M) /S s cm^{-3}	Selectivity $\times 10^4$ (5 M) /S s cm^{-3}
Nafion 212	98.7	18.68	19.82	5.28	4.98
Nafion/GO@PDASA-5	97.2	10.28	12.21	9.46	7.96
Nafion/GO@PDASA-10	97.5	4.08	5.65	23.90	17.26
Nafion/GO@PDASA-20	96.6	1.32	1.53	73.18	63.14
Nafion/GO@PDASA-30	95.3	1.26	1.49	75.64	63.96
Nafion/GO@PDASA-40	96.1	1.23	1.35	78.13	71.19
Nafion/GO -20	86.7	12.56	15.87	6.90	5.46

[a] and [b] are measured at 2 M and 5 M methanol solution, respectively.

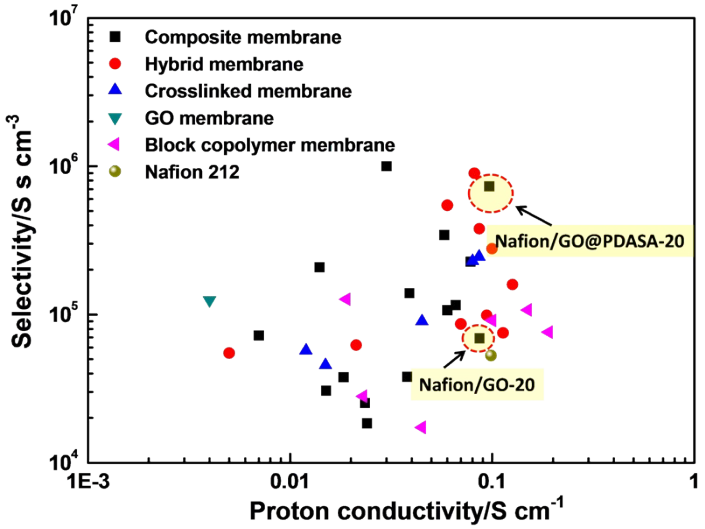

Fig. S7. Comparison of proton conductivity *versus* selectivity for membranes in literature and in this study.

The data can be seen from Table S2. The selectivity is an important parameter to evaluate the potential performance of the membrane in DMFC.[46] Apparently, the Nafion/GO@PDASA-20 membrane exhibits both high proton conductivity and high selectivity, which are the desired properties for high-performance fuel cells.

Reference:

1. W. S. Hummers and R. E. Offeman, *J. Am. Chem. Soc.*, 1958, **80**, 1339-1339.
2. K. Cao, Z. Jiang, J. Zhao, C. Zhao, C. Gao, F. Pan, B. Wang, X. Cao and J. Yang, *J. Membr. Sci.*, 2014, **469**, 272-283.
3. H. W. Kim, H. W. Yoon, S. M. Yoon, B. M. Yoo, B. K. Ahn, Y. H. Cho, H. J. Shin, H. Yang, U. Paik, S. Kwon, J. Y. Choi and H. B. Park, *Science*, 2013, **342**, 91-95.
4. S. Park, D. A. Dikin, S. T. Nguyen and R. S. Ruoff, *J. Phys. Chem. C*, 2009, **113**, 15801–15804.
5. G. He, Z. Li, Y. Li, Z. Li, H. Wu, X. Yang and Z. Jiang, *ACS Appl. Mater. Interfaces*, 2014, **6**, 5362-5366.
6. Z. Li, G. He, B. Zhang, Y. Cao, H. Wu, Z. Jiang and Z. Tiantian, *ACS Appl. Mater. Interfaces*, 2014, **6**, 9799-9807.
7. S. Wang, Y. Liu, S. Huang, H. Wu, Y. Li, Z. Tian and Z. Jiang, *J Membr. Sci.*, 2014, **460**, 62–70.
8. S. Mondal, S. Soam and P. P. Kundu, *J. Membr. Sci.*, 2015, **474**, 140-147.
9. J.-C. Tsai, H.-P. Cheng, J.-F. Kuo, Y.-H. Huang and C.-Y. Chen, *J. Power*

Sources, 2009, **189**, 958-965.
10. Z. Li, Z. Jiang, H. Tian, S. Wang, B. Zhang, Y. Cao, G. He, Z. Li and H. Wu, *J. Power Sources*, 2015, **288**, 384-392.
11. M. Yang, S. Lu, J. Lu, S. P. Jiang and Y. Xiang, *Chem. Commun.*, 2010, **46**, 1434-1436.
12. B. T. McGrail, B. J. Rodier and E. Pentzer, *Chem. Mater.*, 2014, **26**, 5806-5811.
13. C. F. Kins, E. Sengupta, A. Kaltbeitzel, M. Wagner, I. Lieberwirth, H. W. Spiess and M. R. Hansen, *Macromolecules*, 2014, **47**, 2645-2658.
14. S. P. Jiang, Z. Liu and Z. Q. Tian, *Adv. Mater.*, 2006, **18**, 1068-1072.
15. S. Li, S. Zhang, Q. Zhang and G. Qin, *Chem. Commun.*, 2012, **48**, 12201-12203.
16. H. Deligöz, S. Yılmaztürk, T. Karaca, H. Özdemir, S. N. Koç, F. Öksüzömer, A. Durmuş and M. A. Gürkaynak, *J. Membr. Sci.*, 2009, **326**, 643-649.
17. S. Yılmaztürk, H. Deligöz, M. Yılmazoğlu, H. Damyan, F. Öksüzömer, S. N. Koç, A. Durmuş and M. Ali Gürkaynak, *J. Power Sources*, 2010, **195**, 703-709.
18. S. Zhong, X. Cui, T. Fu and H. Na, *J. Power Sources*, 2008, **180**, 23-28.
19. M. M. Mannarino, D. S. Liu, P. T. Hammond and G. C. Rutledge, *ACS Appl. Mater. Interfaces*, 2013, **5**, 8155-8164.
20. J. Wang, L. Xiao, Y. Zhao, H. Wu, Z. Jiang and W. Hou, *J. Powe r Sources* **192**, 336–343.
21. Y. Zhang, W. Cai, F. Si, J. Ge, L. Liang, C. Liu and W. Xing, *Chem. Commun.*, 2012, **48**, 2870-2872.
22. L. Sha Wang, A. Nan Lai, C. Xiao Lin, Q. Gen Zhang, A. Mei Zhu and Q. Lin Liu, *J. Membr. Sci.*, 2015, **492**, 58-66.
23. T. Yuan, L. Pu, Q. Huang, H. Zhang, X. Li and H. Yang, *Electrochim. Acta*, 2014, **117**, 393-397.
24. C. W. Lin and Y. S. Lu, *J. Power Sources*, 2013, **237**, 187-194.
25. Z. Jiang, X. Zhao, Y. Fu and A. Manthiram, *J. Mater. Chem.* , 2012, **22**, 24862.
26. B. G. Choi, J. Hong, Y. C. Park, D. H. Jung, W. H. Hong, P. T. Hammond and H. Park, *ACS nano*, 2011, **5**, 5167–5174.
27. M. M. Hasani-Sadrabadi, E. Dashtimoghadam, F. S. Majedi, K. Kabiri, M. Solati-Hashjin and H. Moaddel, *J. Membr. Sci.*, 2010, **365**, 286-293.
28. M.-K. Song, S.-B. Park, Y.-T. Kim, K.-H. Kim, S.-K. Min and H.-W. Rhee, *Electrochim. Acta*, 2004, **50**, 639-643.
29. Y.-F. Lin, C.-Y. Yen, C.-H. Hung, Y.-H. Hsiao and C.-C. M. Ma, *J. Power Sources*, 2007, **168**, 162-166.
30. Z. Chai, C. Wang, H. Zhang, C. M. Doherty, B. P. Ladewig, A. J. Hill and H. Wang, *Adv. Funct. Mater.*, 2010, **20**, 4394-4399.
31. Y. Cui, A. P. Baker, X. Xu, Y. Xiang, L. Wang, M. Lavorgna and J. Wu, *J. Power Sources*, 2015, **294**, 369-376.
32. G. He, L. Nie, X. Han, H. Dong, Y. Li, H. Wu, X. He, J. Hu and Z. Jiang, *J. Power Sources*, 2014, **259**, 203-212.
33. K. Ahn, M. Kim, K. Kim, H. Ju, I. Oh and J. Kim, *J. Power Sources*, 2015, **276**,

309-319.
34. L. Li, J. Zhang and Y. Wang, *J. Membr. Sci.*, 2003, **226**, 159-167.
35. W. H. Lee, K. H. Lee, D. W. Shin, D. S. Hwang, N. R. Kang, D. H. Cho, J. H. Kim and Y. M. Lee, *J. Power Sources*, 2015, **282**, 211-222.
36. J. Ren, S. Zhang, Y. Liu, Y. Wang, J. Pang, Q. Wang and G. Wang, *J. Membr. Sci.*, 2013, **434**, 161-170.
37. C. Fang, D. Julius, S. W. Tay, L. Hong and J. Y. Lee, *J. Phys. Chem. B*, 2012, **116**, 6416-6424.
38. D. S. Kim, H. B. Park, J. W. Rhim and Y. M. Lee, *Solid State Ionics*, 2005, **176**, 117-126.
39. J.-W. Rhim, H. B. Park, C.-S. Lee, J.-H. Jun, D. S. Kim and Y. M. Lee, *J. Membr. Sci.*, 2004, **238**, 143-151.
40. A. Paneri, Y. Heo, G. Ehlert, A. Cottrill, H. Sodano, P. Pintauro and S. Moghaddam, *J. Membr. Sci.*, 2014, **467**, 217-225.
41. Q. Li, Y. Chen, J. R. Rowlett, J. E. McGrath, N. H. Mack and Y. S. Kim, *ACS Appl. Mater. Interfaces*, 2014, **6**, 5779-5788.
42. J. Kim, B. Kim and B. Jung, *J. Membr. Sci.*, 2002, **207**, 129-137.
43. B. Kim, J. Kim and B. Jung, *J. Membr. Sci.*, 2005, **250**, 175-182.
44. Y. A. Elabd, E. Napadensky, J. M. Sloan, D. M. Crawford and C. W. Walker, *J. Membr. Sci.*, 2003, **217**, 227-242.
45. G. He, Z. Li, J. Zhao, S. Wang, H. Wu, M. D. Guiver and Z. Jiang, *Adv. Mater.*, 2015, DOI: 10.1002/adma.201501406.
46. S. K. Nataraj, C. H. Wang, H. C. Huang, H. Y. Du, S. F. Wang, Y. C. Chen, L. C. Chen and K. H. Chen, *ChemSusChem*, 2012, **5**, 392-395.